ADVANCED FUNCTIONAL MATERIALS

Supporting Information

for *Adv. Funct. Mater.,* DOI: 10.1002/adfm.202209748

Protease-Activatable Nanozyme with Photoacoustic and Tumor-Enhanced Magnetic Resonance Imaging for Photothermal Ferroptosis Cancer Therapy

*Wen Qin, Jinzhao Huang, Chunsheng Yang, Quer Yue, Shizhen Chen, Mengdie Wang, Shangbang Gao, Xin Zhou, Xiangliang Yang, and Yan Zhang**

Supporting Information

Protease-activatable nanozyme with photoacoustic and tumor-enhanced magnetic resonance imaging for photothermal ferroptosis cancer therapy

*Wen Qin,[a#] Jinzhao Huang,[a#] Chunsheng Yang,[b] Quer Yue,[b] Shizhen Chen,[b] Mengdie Wang,[c] Shangbang Gao,[a] Xin Zhou,[b] Xiangliang Yang,[a,d] and Yan Zhang[*a,d]*

[a.] National Research Centre for Nanomedicine, College of Life Science and Technology, Huazhong University of Science and Technology, Wuhan, P. R. China, 430074.

[b.] State Key Laboratory of Magnetic Resonance and Atomic and Molecular Physics National Center for Magnetic Resonance in Wuhan, Wuhan Institute of Physics and Mathematics Innovation Academy of Precision Measurement Science and Technology Chinese Academy of Sciences, Wuhan, 430071, P. R. China.

[c.] Department of Neurology, Union Hospital, Tongji Medical College, Huazhong University of Science and Technology, Jiefang Avenue, Wuhan, 430022, P. R. China.

[d.] Hubei Key laboratory of Bioinorganic Chemistry and Materia Medical, Huazhong University of Science and Technology, Wuhan, 430074, P. R. China.

Experimental Section:

Chemicals:

Ferric chloride hexahydrate ($FeCl_3 \cdot 6H_2O$), ethylene glycol, sodium acetate (NaAc), and sodium hydroxide (NaOH) were obtained from Beijing Chemical Reagents Company (China). Gelatin was purchased from Aladdin Reagent Co. Ltd. (Shanghai, China). $CuCl_2 \cdot 2H_2O$, Se powder, sodium borohydride ($NaBH_4$), and MSA were purchased from Sigma-Aldrich. Methoxy poly (ethylene glycol) thiol (mPEG-SH, 5 kD) was purchased from Kaizheng Biotech (Beijing, China). 1-(3-Dimethylaminopropyl)-3-ethylcarbodiimide hydrochloride (EDC), N-Hydroxysuccinimide (NHS) and Methylene blue (MB) was purchased from Aladdin.2,7-dichlorodihydrofluorescein diacetate (DCFH-DA) and lipopolysaccharide (LPS) were bought from Sigma-Aldrich Company (St Louis, MO, USA). GSH assay kit was purchased from Nanjing Jiancheng Bioengineering Institute (Nanjing, China). MMP-2 and red cell lysis solution was purchased from Biosharp (Hefei, China). Cy5 NHS ester was purchased from Ruixi (Xian, China). $BODIPY^{665/676}$ was purchased from Thermo Fisher Scientific. Cell counting kit-8 (CCK-8) was provided by Dojindo Laboratories (Kumamoto, Kyushu, Japan). ATP determination kit, DAPI and lyso-Tracker were purchased from Beyotime Institute of Biotechnology (Shanghai, China). Calreticulin (CRT) Rabbit monoclonal antibody was obtained from Cell Signaling Technology (Danvers, MA, USA). Mouse high mobility group protein B1 (HMGB1) ELISA kit was obtained from ELISA Lab (Wuhan, China). Fetal bovine serum (FBS) and collagenase Type I were obtained from Gibco Life Technologies

(New York, NY, USA). Roswell Park Memorial Institute (RPMI) 1640 medium, PBS and penicillin-streptomycin were purchased from HyClone (Logan, Utah, USA). Recombinant mouse granulocyte macrophage colony-stimulating factor (GM-CSF), IL-4, and IFN-γ were provided by PeproTech (Rocky Hill, NJ, USA). Antibodies used for flow cytometry analysis were purchased from BioLegend (San Diego, CA, USA).

Synthesis of Fe_3O_4 nanoclusters. Fe_3O_4 nanoclusters were synthesized according to the previous report [1]. Gelatin (300 mg) was dissolved in 20 mL of ethylene glycol. Then, $FeCl_3 \cdot 6H_2O$ (324 mg, 1.2 mmol) was dissolved in the above mixture to form a clear solution, followed by addition of NaAc (900 mg). The mixture was stirred vigorously for 30 min, and the pH was adjusted to 7.0 by 1 M NaOH dissolved in ethylene glycol. Then, the mixture was sealed in a Teflon-lined stainless steel autoclave. The reaction was kept at 200 °C for 6 h and allowed to cool to room temperature. The dark brown products were washed several times with water using magnet and dried at 60 °C.

Synthesis of $Cu_{1.77}Se$ nanoparticles. $Cu_{1.77}Se$ nanoparticles were also synthesized according to the previous report [2]. In a typical synthesis, 39.48 mg (0.5 mmol) Se powder was reduced by 56.75 mg (1.5 mmol) $NaBH_4$ in 50 mL H_2O under magnetic stirring at room temperature with the protection of Argon gas. 0.17 mg (1 mmol) $CuCl_2 \cdot 2H_2O$ and 1 g (6.66 mmol) MSA were completely dissolved in 5 mL distilled water and afterwards, was added into the selenium precursor solution to generate the $Cu_{1.77}Se$. After purified by ultra-filtration at 5000 rpm using a membrane with a molecular weight cutoff of 30 kDa, the $Cu_{1.77}Se$ was obtained and stored at 4 °C for

further characterization and use.

To synthesize $Cu_{1.77}Se$-PEG, 0.2 g PEG-SH was added to modify the surfaces of the MSA-capped $Cu_{1.77}Se$ NPs at room temperature. After stirring for 12h, the mixtures were purified by a similar ultrafiltration method and then dialyzed against distilled water to remove free PEG-SH. The obtained $Cu_{1.77}Se$-PEG was stored at 4 °C for further use.

Synthesis of Fe_3O_4@$Cu_{1.77}Se$ nanozymes. $Cu_{1.77}Se$ (1.0, 3.0, 5.0, 7.0 mg) was activated by EDC for 20 min in 10 mL MES buffer (pH 5.5) at room temperature. Then, Fe_3O_4 (1.0 mg) and NHS were added into the above solution and stirred for 12 h at room temperature with the protection of Argon gas. The mixtures were washed several times with water using magnet. HS-PEG was used to modify the surface of the Fe_3O_4@$Cu_{1.77}Se$. Dialysis (MW: 3500) was used to remove the excess reagents.

Characterization: The morphologies of Fe_3O_4, $Cu_{1.77}Se$, and Fe_3O_4@$Cu_{1.77}Se$ nanoparticles were characterized by transmission electron microscope (HITACHI HT7700, Japan). High resolution transmission electron microscope (HRTEM) images and elemental mapping were recorded on Tecnai G^2 F30 (FEI, Holland) equipped with X-ray energy dispersive spectrometer. X-ray powder diffraction of Fe_3O_4@$Cu_{1.77}Se$ were performed on X'pert3 powder (PANalytical, Holland) with Cu $K\alpha$ radiation (λ =1.54184 Å). XPS measurements were carried out on an AXIS-ULTRA DLD-600W instrument (Shimadzu, Japan). The magnetic properties were measured at 300 K on a MPMS3 system alternating gradient magnetometer (Quantum Design Corporation, San Diego, USA). FTIR spectra were conduct on VERTEX 70 (Bruker, German). The

hydrodynamic diameters and zeta-potentials were measured by Zetasizer Nano ZS90 (Malvern, UK). TGA was performed to analyze the weights of surface ligands at a heating rate of 10 °C min^{-1} from room temperature to 580 °C under argon atmosphere on Diamond TG/DTA (PerkinElmer Instruments). Ultraviolet-visible-near-infrared spectra were recorded with a SolidSpec-3700 UV-vis-NIR spectrophotometer (Shimadzu, Japan).

Photothermal performance of Fe_3O_4@$Cu_{1.77}Se$ in aqueous solution. To investigate the photothermal performance of Fe_3O_4@$Cu_{1.77}Se$ in solution, DI water and Fe_3O_4@$Cu_{1.77}Se$ with different concentrations (12.5, 25, 50 and 100 μg mL^{-1}) were illuminated for 10 min by a continuous 1064 nm laser (0.75 and 1.0 W cm^{-2}). Moreover, five laser on/off cycles were used to evaluate the photothermal stability of Fe_3O_4@$Cu_{1.77}Se$. The temperature of the solutions was monitored by an IR thermal camera (FLIR E8, USA).

The photothermal conversion efficiency (η) of Fe_3O_4@$Cu_{1.77}Se$ was calculated according to the previous report [3]. 1 ml of 50 μg mL^{-1} Fe_3O_4@$Cu_{1.77}Se$ solution was added into a cuvette and irradiated by 1064 nm laser for 10 min, then naturally cooling after the laser turned off. η is calculated according to the following equation.

$$\eta = \frac{m \cdot c \cdot (T_{max} - T_{max,H2O})}{I \cdot (1 - 10^{-A}) \cdot \tau_s}$$

m is the solution mass, c is the heat capacity of water and equal to 4.2 J/g, T_{max} and T_{max,H_2O} are the maximum temperatures by Fe_3O_4@$Cu_{1.77}Se$ solution and water, respectively. I is the laser power and equal to 0.75 W cm^{-2} in the study. A is the absorbance of the nanoparticle solution at 1064 nm, and τ_s is the system time constant,

according to the linear regression of the cooling profile. The photothermal conversion efficiency is calculated to be 67.6% by using these parameters.

Hydroxyl radical (·OH) generation measurement of Fe_3O_4@$Cu_{1.77}Se$ in solution. Detection of the generation of ·OH by nanoparticles with different treatments was conducted using MB as indicator[4]. Briefly, Fe_3O_4 (300 μg mL^{-1}), $Cu_{1.77}Se$ (250 μg mL^{-1}) or Fe_3O_4@$Cu_{1.77}Se$ (250 μg mL^{-1}) was pretreated with MMP-2 solution (10 μg mL^{-1} in PBS) or without MMP-2 for 0 h, 24 h and 48 h at 37 °C, respectively, followed by the addition of H_2O_2 (5 mM) and MB (20 μg mL^{-1}) into the solution. The absorbance of MB at 664 nm were recorded every two minutes to qualify the generation of ·OH. Finally, Fe_3O_4@$Cu_{1.77}Se$ pretreated with MMP-2 solution for 48 h were irradiated by a 1064 nm laser at 0.75 W cm^{-2} for 10 min, followed by the H_2O_2 (5 mM) and MB (20 μg mL^{-1}) into the solution. The absorbance of MB at 664 nm was monitored every two minutes to qualify the generation of ·OH. The catalytic efficacy of Fe_3O_4@$Cu_{1.77}Se$ were determined by incubation the nanozymes with different concentration of H_2O_2 in the presence of MMP-2 at 0 h and 48 h, respectively. Afterwards, the absorbance of MB at 664 nm was monitored to qualify the *K*m and *V*m.

GSH measurement of Fe_3O_4@$Cu_{1.77}Se$ in solution. Fe_3O_4@$Cu_{1.77}Se$ and Fe_3O_4@$Cu_{1.77}Se$+MMP-2 were stirred for 0 h, 24 h and 48 h at 37 °C respectively. Then, Fe_3O_4+MMP and $Cu_{1.77}Se$+MMP-2 were stirred for 48 h at 37 °C, respectively. Fe_3O_4@$Cu_{1.77}Se$, Fe_3O_4 were at the Fe concentration of 300 μg mL^{-1}. and $Cu_{1.77}Se$ was at the Cu concentration of 250 μg mL^{-1}. MMP-2 was 10 μg mL^{-1} in PBS. 5 μM

GSH was added to the above suspensions and incubated at 37 °C for 40 min. The GSH content was determined by GSH assay kit according to the manufacturer's guidance. Finally, Fe_3O_4@$Cu_{1.77}$Se+MMP-2 (48 h), 5 μM GSH were irradiated by a 1064 nm laser at 0.75 W cm^{-2} for 10 min. The GSH content was determined by GSH assay kit every two minutes.

Cell culture: Murine breast cancer 4T1 cells and murine RAW264.7 macrophages were purchased from Type Culture Collection of the Chinese Academy of Sciences (Shanghai, China). 4T1 cells were cultured in complete RPMI-1640 medium and RAW264.7 macrophages in complete DMEM medium. The complete mediums contained 10% FBS, penicillin (100 U mL^{-1}) and streptomycin (100 μg mL^{-1}). RAW264.7 cells were stimulated by LPS (100 ng mL^{-1}) and IFN-γ (20 ng mL^{-1}) for 1 day to acquire M1-like macrophages and stimulated by IL-4 (20 ng mL^{-1}) to acquire M2-like macrophages. Bone marrow-derived DCs (BMDCs) were obtained from 6-week-old BALB/c female mice as described.[5] BMDCs were cultured in complete RPMI 1640 medium containing GM-CSF (20 ng mL^{-1}) and IL-4 (20 ng mL^{-1}) for 5 days to acquire the immature DCs. All cells were cultured at 37 °C in a 5% CO_2 incubator.

Cellular uptake assay: To detect the cellular uptake, 4T1 cells were treated with Fe_3O_4@$Cu_{1.77}$Se-Cy5 at the Fe concentration of 50 μg mL^{-1} for 0, 2, 4, 6 h. The cells were washed with PBS three times and collected for flow cytometric analysis (Cytoflex S, Beckman Coulter).

Cellular co-localization: 4T1 cells were seeded into confocal-well culture plates at

the density of 1×10^4/well, and incubated at 37 ℃ for 24 h. Then, 50 μg mL^{-1} Fe_3O_4@$Cu_{1.77}$Se-Cy5 was added and further incubated for 4 h. Subsequently, the fluorescence images of the cells were obtained by CLSM after staining with Lyso-Tracker (Ex: 543 nm, Em: 590 nm) and DAPI (Ex: 405 nm, Em: 460 nm).

Cellular toxicity of Fe_3O_4@$Cu_{1.77}$Se: 4T1 cells were seeded into 96-well culture plates at the density of 1×10^4/well, followed by incubation with Fe_3O_4@$Cu_{1.77}$Se at different concentration (0, 25, 50, 100 μg mL^{-1}) for 24 h. The cell viability was evaluated by CCK-8 assay based on the absorbance at 450 nm with microplate reader (Thermofisher NanoDrop 2000, USA).

***In vitro* cell viability evaluation:** 4T1 cells were seeded into 96-well culture plates at the density of 1×10^4/well, and incubated for 24 h. After replacing the culture medium with fresh medium containing 5 mM H_2O_2, the cells were divided into twelve groups with treatments: group 1: PBS, group 2: PBS+MMP-2, group 3: PBS+MMP-2+Laser, group 4: Fe_3O_4, group 5: Fe_3O_4+MMP-2, group 6: Fe_3O_4+MMP-2+Laser, group 7: $Cu_{1.77}$Se, group 8: $Cu_{1.77}$Se+MMP-2, group 9: $Cu_{1.77}$Se+MMP-2+Laser, group 10: Fe_3O_4@$Cu_{1.77}$Se, group 11: Fe_3O_4@$Cu_{1.77}$Se+MMP-2, group 12: Fe_3O_4@$Cu_{1.77}$Se+MMP-2+Laser. After incubation for 4 h, the cells in group 6, 9 and 12 were further exposed to 1064 nm photoirradiation (0.75 W cm^{-2}, 4 min), followed by continuously incubation for 20 h. Subsequently, cell viability was evaluated by CCK-8 assay based on the absorbance at 450 nm with microplate reader (Thermofisher NanoDrop 2000, USA).

ROS detection *in vitro*: 4T1 cells were seeded into confocal-well culture plates at the

density of 1×10^4/well, and incubated at 37 ℃ for 24 h. Then, the cells were divided into 12 groups and treated by the above-mentioned manners. After incubation for 4 h, the cells in group 6, 9 and 12 were exposed to 1064 nm photoirradiation (0.75 W cm^{-2}, 4 min) with further incubation for 4 h. DCFH-DA (20 μM) were added into 4T1 cells and incubated for 30 min. Afterwards, cells were washed with ice-cold PBS three times, and the fluorescence images were recorded by CLSM (Ex: 504 nm, Em: 529 nm), and the mean fluorescence intensity of each image were counted with Image J software.

GSH depletion *in vitro*: 4T1 cells were seeded into confocal-well culture plates at the density of 1×10^4/well, and incubated at 37 ℃ for 24 h. Then the cells were divided into 12 groups and treated by the above-mentioned manners. After incubation for 4 h, the cells of group 6, 9 and 12 were exposed to 1064 nm laser irradiation (0.75 W cm^{-2}, 4 min) and continuously incubated for 4 h. Subsequently, the medium was removed and cells were washed with ice-cold PBS three times. Then, 80 μL of Triton-X-100 lysis buffer (0.4%) was added to lyse the cells obtained. GSH content was determined by GSH assay kit according to the manufacturer's guidance.

Examination of LPO *in vitro*: 4T1 cells were seeded into confocal-well culture plates at the density of 1×10^4/well, and incubated at 37 ℃ for 24 h. The cells were divided into 12 groups and treated by the above-mentioned manners. After incubation for 4 h, the cells of group 6, 9 and 12 were exposed to 1064 nm photoirradiation (0.75 W cm^{-2}, 4 min) and further incubated for 12 h. Cells were then washed with PBS, followed by staining with $BODIPY^{665/676}$ (10 μM, 30 min) and DAPI. Subsequently,

cells were washed three times in ice-cold PBS, and the fluorescence images were recorded by CLSM (Ex: 665 nm, Em: 676 nm) and the mean fluorescence intensity of each image were counted with Image J software.

Penetration evaluation of Fe_3O_4@$Cu_{1.77}$Se nanozymes in 3D tumor spheroids: 4T1 multicellular tumor spheroids were developed after seeding single cells in fibrin gels[6]. After 5 days growth, the tumor spheroids were incubated in RPMI 1640 medium containing Fe_3O_4@$Cu_{1.77}$Se-Cy5 (50 μg mL^{-1}) and Fe_3O_4@$Cu_{1.77}$Se-Cy5 (50 μg mL^{-1}) + MMP-2 for 4 h. Then, Fe_3O_4@$Cu_{1.77}$Se-Cy5 + MMP-2 nanoparticles received 1064 nm laser irradiation (0.75 W cm^{-2}, 4 min) and further incubation for 6 h. Subsequently, the spheroids were harvested, washed with ice-cold PBS three times. The fluorescence of Fe_3O_4@$Cu_{1.77}$Se-Cy5 was detected using Z-stack imaging using an Olympus FV3000 confocal microscope, with 10 μm intervals from the top of spheroids to the middle. The fluorescence of Fe_3O_4@$Cu_{1.77}$Se-Cy5 was analyzed using Image J software.

Western blot analysis of ferroptosis and apoptosis: 4T1 cells were seeded into 6-well culture plates at 5×10^5/well, and incubated at 37 ℃ for 24 h. Then, 12 groups including PBS, Fe_3O_4@$Cu_{1.77}$Se, Fe_3O_4@$Cu_{1.77}$Se+MMP-2, PBS+laser, Fe_3O_4@$Cu_{1.77}$Se+laser, Fe_3O_4@$Cu_{1.77}$Se+MMP-2 +laser at the Fe concentration of 50 μg mL^{-1} dispersed in FBS free culture medium with 5 mM H_2O_2 were added into the plates and further incubated for 4 h. Photoirradiation (0.75 W cm^{-2}, 4 min) were applied, followed by incubation for another 16 h. Then, RIPA lysis buffer containing phenylmethanesulfonylfluoride (PMSF) was added and incubated on ice for 1 h. Then,

the mixture was centrifuged to extract proteins from the supernatant. Protein concentration was determined by the bicinchoninic acid (BCA) protein assay kit (Beyotime). Equal amount of protein of each sample was electrophoresed on polyacrylamide gel (10%), and transferred onto a nitrocellulose membrane. After blocking in 5% BSA solution, the blot was incubated at 4 ℃ with diluted primary antibodies (caspase-3, GPX4, ACSL4, FPN-1, ferritin and GAPDH) purchased from ABclonal (China). All above antibodies were diluted at 1:1000. The membrane was washed three times with TBST buffer and incubated with goat anti-rabbit IgG antibody diluted at 1:3000 for cleaved caspase-3, GPX 4, ACSL 4, FPN-1, ferritin, and goat anti-mouse IgG antibody diluted at 1:3000 for GAPDH. Afterwards, the proteins were measured by chemiluminescence imaging system (Bio-Rad ChemiDoc XRS+, USA).

Detection of immunogenic cell death of 4T1 cells *in vitro*: 4T1 cancer cells were seeded into 24-well culture plates at the density of 1×10^5/well, and incubated at 37 ℃ for 24 h. Then, the cells were divided into 12 groups and treated in the above-mentioned manners. After incubation for 4 h, the cells in group 6, 9 and 12 were exposed to 1064 nm photoirradiation (0.75 W cm^{-2}, 4 min) and continuously incubated for 12 h. Afterwards, the level of CRT was measured by flow cytometry. The concentration of HMGB1 and ATP were qualified by ELISA kits.

Inducing DC maturation *in vitro*: 4T1 cancer cells were seeded into 24-well culture plates at the density of 1×10^5/well, and incubated at 37 ℃ for 24 h. Then the cells were divided into 12 groups and treated by the above-mentioned manners. After

incubation for 4 h, the cells in group 6, 9 and 12 were exposed to 1064 nm photoirradiation (0.75 W cm^{-2}, 4 min) and continuously incubated for 20 h. Subsequently, 5×10^5 immature DCs were co-cultured with pretreated 4T1 cells for 24 h. After incubation with anti-CD11c-PE/Cy7, anti-CD80-PE, and anti-CD86-APC antibodies, DC maturation was examined by flow cytometry.

M2 macrophage repolarization *in vitro*: 5×10^5 M2-like macrophages were co-cultured with respective nanoparticle pretreated 4T1 cells for 24 h. After staining with anti-CD11b-FITC, anti-F4/80-PC7, anti-CD206-APC, anti-CD86-PE antibodies, cells were examined by flow cytometry.

Tumor models: BALB/c female mice (6~8 weeks old, 15~18 g) were purchased from Vital River Laboratory (Beijing, China). Animal protocols were performed under the guidelines for human and responsible use of animals in research set by Huazhong University of Science and Technology. For the tumor inoculation, 4T1 cells at the density of 1×10^6 and 4×10^5 suspended in PBS were subcutaneously injected into the right and left flank of female BALB/c mice, respectively. The tumor-bearing mice received treatments after the tumor reached the proper size.

MR/PA imaging measurement: For MR imaging, Fe_3O_4@$Cu_{1.77}Se$ solutions with different Fe concentrations of 0, 0.03, 0.08, 0.12, 0.23, 0.45 mM and Fe_3O_4@$Cu_{1.77}Se$+MMP-2 (10 μg mL^{-1}, 48 h) solutions with different Fe concentrations of 0, 0.03, 0.12, 0.17, 0.32, 0.40 mM were prepared for *in vitro* MRI signals collection. Primary tumors of mice were intratumorally injected with Fe_3O_4@$Cu_{1.77}Se$ (20 μL, 2 mg mL^{-1}) after the tumors grown to about 100 mm^3. At 0,

10 and 20 h, the mice were mount for MR imaging. T_2-weighted MR images and relaxation time measurements were performed on a 7 T micro-imaging system (Bruker Avance 400, Ettlingen, Germany) (TR = 3000 ms, TE = 50 ms). As for *in vivo* MR imaging, the tumor-bearing mice were intravenously injected with 120 μL of 2 mg mL^{-1} $Fe_3O_4@Cu_{1.77}Se$. A permanent magnet was located at the primary tumor site. At 0, 6, 12 and 24 h, MRI measurements were carried out.

For PA imaging, $Fe_3O_4@Cu_{1.77}Se$ and $Fe_3O_4@Cu_{1.77}Se$+MMP-2 (10 μg mL^{-1}, 48 h) solutions with Cu concentrations of 0.12, 0.23, 0.45, 0.65, 0.90 mM were prepared for *in vitro* PA signals collection. To evaluate the PA imaging performance *in vivo*, mice were intravenously injected with 120 μL of $Fe_3O_4@Cu_{1.77}Se$ with a concentration of 2 mg mL^{-1}. A permanent magnet was located at the primary tumor site. At 0, 6, 12 and 24 h, the mice were mount for PA imaging using a MSOT in Vision 256-TF small animal imaging system (iThera Medical GmbH, Munich, Germany).

Antitumor studies *in vivo*: To evaluate the antitumor efficacy of $Fe_3O_4@Cu_{1.77}Se$ *in vivo*, 4T1 tumor models were established. For the tumor inoculation, 4T1 cells at the density of 1×10^6 and 4×10^5 suspended in PBS were subcutaneously injected into the right and left flank of female BALB/c mice, respectively. When the right (primary) tumor volume reached 100 mm^3, the mice were randomly divided into eight groups: PBS, Fe_3O_4, $Cu_{1.77}Se$, $Fe_3O_4@Cu_{1.77}Se$, PBS+laser, Fe_3O_4+laser, $Cu_{1.77}Se$+laser, $Fe_3O_4@Cu_{1.77}Se$+laser. Mice were intravenously injected with 120 μL of Fe_3O_4, $Cu_{1.77}Se$ and $Fe_3O_4@Cu_{1.77}Se$ with concentration of 2 mg mL^{-1}. The primary tumor

was treated with a permanent magnet and the left (distant) tumor without magnet. Photoirradiation (1064 nm, 0.75 W cm^{-2}, 10 min) was conducted at 12 h post-injection. Body weight and tumor volume of mice were recorded every other day. The tumor volume (V) was calculated according to the formula: $V=(L\times W^2)/2$, while L and W were the longest and shortest diameter of the tumor, respectively.

Evaluation of lung metastasis: After 14 days treatments, the lungs of mice were harvested (n=6). Three of them were stabilized in Bouin's solution to count the number of metastatic nodes, and the rest (n=3) were fixed in 4% neutral paraformaldehyde solution for H&E staining. The lung tissue sections were imaged by optical microscopy (Leica, DM 3000).

Evaluation of metastasis-related protein expression. After treatments for 5 days, mice in each group were euthanized and tumors were extracted. The tumors were used for imaging and quantification of metastasis-related protein, including HGF, MTA2 and VCAM-1, using anti-HGF antibodies, anti-MTA2 antibodies and anti-VCAM-1 antibodies according to the previous protocols[7]. The obtained fluorescence images were obtained by fluorescence microscope (Nikon Eclipse TI-SR, Japan), and quantified with Image J software.

Intratumoral distribution *in vivo*: 4T1 tumor tissues were excised from pretreated 4T1 tumor-bearing mice. Mice were intravenously injected with 120 μL of Fe_3O_4@$Cu_{1.77}$Se-Cy5 with a concentration of 2 mg mL^{-1}. At 12 h, the primary tumors were treated with laser irradiation (1064 nm, 0.75 W cm^{-2}, 10min) and the distant tumors without laser irradiation. After one day, 4T1 tumor tissues were collected and

fixed in 4% neutral paraformaldehyde solution. Then, CD31 immunohistochemical staining was conduct after they were embedded in paraffin for sectioning with the thickness of 5 μm at depth of 3 mm in the direction of laser irradiation (photothermal depth). The section images were obtained by fluorescence microscope (Nikon Eclipse TI-SR, Japan). The distribution of Fe_3O_4@$Cu_{1.77}Se$-Cy5 fluorescence from the blood vessels to the distant was analyzed using Image J software.

***In vivo* measurements of ROS generation:** At 12 h post-injection of PBS, Fe_3O_4, $Cu_{1.77}Se$, Fe_3O_4@$Cu_{1.77}Se$ (2 mg mL^{-1}, 120 μL), mice were intratumorally injected of DCFH-DA with or without 1064 nm photoirradiation (0.75 W cm^{-2}, 10 min). After photoirradiation, the mice were euthanized and tumors were immediately harvested. The tumor tissues were fixed in 4% paraformaldehyde and then cut into 5-μm sections followed by staining with DAPI. The fluorescence images of DCFH-DA were obtained by fluorescence microscope (Nikon Eclipse TI-SR, Japan), and quantified with Image J software.

***In vivo* evaluation of ferroptosis/apoptosis-related biomarkers:** After 2 days of treatments, LPO staining with $BODIPY^{665/676}$ and immunofluorescence staining of GPX4, ACSL4 and caspase-3 were performed following the same procedure as the above-described ferroptosis/apoptosis staining. Fluorescence imaging was conducted using the LSM800 confocal laser scanning microscope. The respective fluorescence images by each antibody were obtained by fluorescence microscope (Nikon Eclipse TI-SR, Japan), and quantified with Image J software.

Detection of ICD-related proteins *in vivo*: The mice were sacrificed on the fifth day

after treatments and the tumors were excised for evaluation of ICD related proteins. Tumors were fixed in 4% neutral paraformaldehyde solution. Cryo-sections of 5 μm were performed followed by staining with HMGB1 and CRT antibodies, respectively. The fluorescence images were obtained by fluorescence microscope (Nikon Eclipse TI-SR, Japan), and quantified with Image J software.

Detection of DCs maturation *in vivo*: On the fifth day after treatments, the tumor-draining lymph nodes were excised for evaluation of DCs maturation. Maturation of DCs was evaluated using flow cytometry followed by staining with anti-CD11c-PE/Cy7, anti-CD80-PE and anti-CD86-APC antibodies.

Tumor immune microenvironment analysis *in vivo*: On the fifth day after treatments, the tumors were harvested, digested by collagenase I for 30 min at 37 ℃, and then, grounded. The erythrocyte lysate was afterwards applied to remove the red blood cells. The single-cell suspension was collected after filtration by nylon mesh filters. For CTLs analysis, cells were stained with antiCD45-APC/Cy7, anti-CD3-FITC, Brilliant Violet 421 anti-CD4 and anti-CD8a-PE/Cy7 antibodies. For M1/M2-like TAMs analysis, cells were stained with anti-CD11b-FITC, anti-F4/80-PC7, anti-CD206-APC and anti-CD86-PE antibodies. Then, cells were quantified by flow cytometry.

Cytokine detection: For cytokine detection, mice blood was collected *via* the retro-orbital plexus on day 14 and the serum was harvested by centrifuging. IFN-γ and TNF-α in serum were quantified by ELISA kits.

Histological studies: After treatments for 14 days, the mice were sacrificed. The

tumors, hearts, livers, spleens and kidneys were fixed in 4% neutral paraformaldehyde solution. Then, tunnel and H&E staining were conduct after they were embedded in paraffin for sectioning with the thickness of 5 μm. The section images were obtained by optical microscopy (Leica, DM 3000).

Statistical analysis：GraphPad Prism software was used to analyze and present the data, which showed as mean±standard error of the mean (SEM). Statistical comparisons were assessed by two-way ANOVA. The accepted level of significance was $P^* < 0.05$. $P^{**} < 0.01$, $P^{***} < 0.001$.

Supplementary Figures:

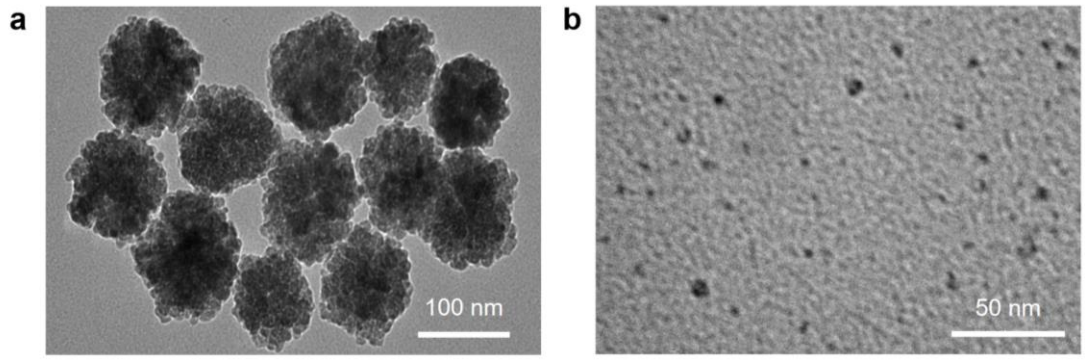

Figure S1. TEM images of (a) Fe_3O_4 and (b) $Cu_{1.77}Se$ nanoparticles.

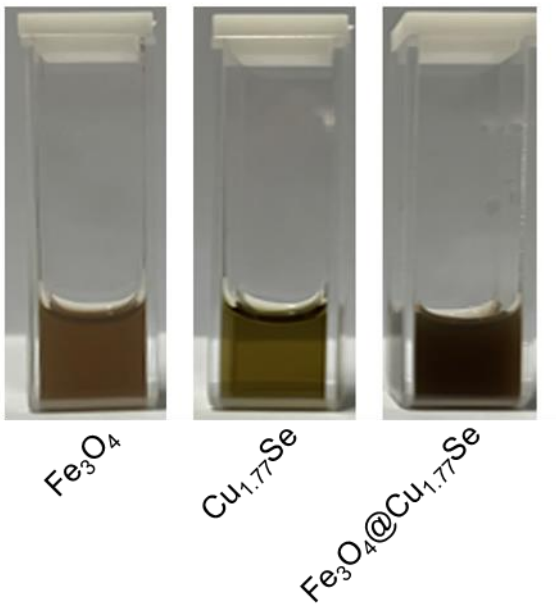

Figure S2. Digital images of Fe_3O_4, $Cu_{1.77}Se$ and $Fe_3O_4@Cu_{1.77}Se$ nanozymes.

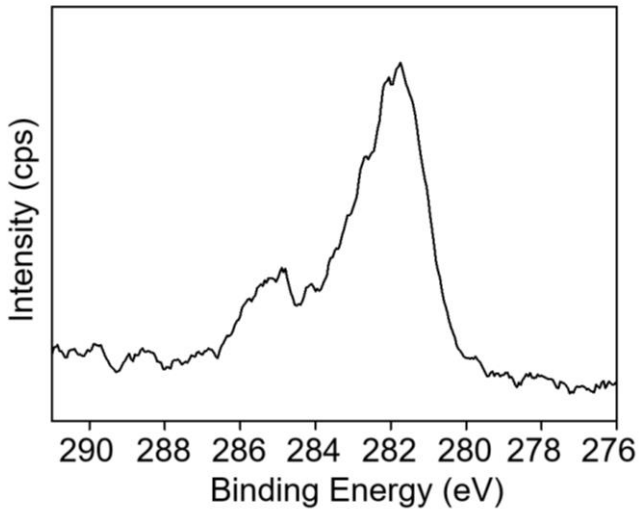

Figure S3. XPS spectra of Se in $Fe_3O_4@Cu_{1.77}Se$ nanozymes.

	Fe/Cu (molar ratio)
$Fe_3O_4@Cu_{1.9}Se$	1:0.83

Table S1. Molar ratio of $Fe_3O_4@Cu_{1.77}Se$ nanozymes measured by ICP-OES.

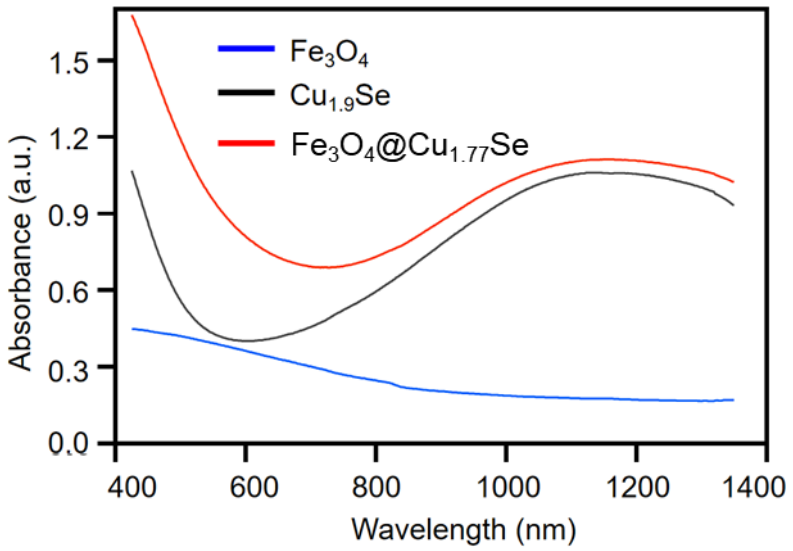

Figure S4. UV-visible-NIR spectra of Fe_3O_4, $Cu_{1.77}Se$ and $Fe_3O_4@Cu_{1.77}Se$.

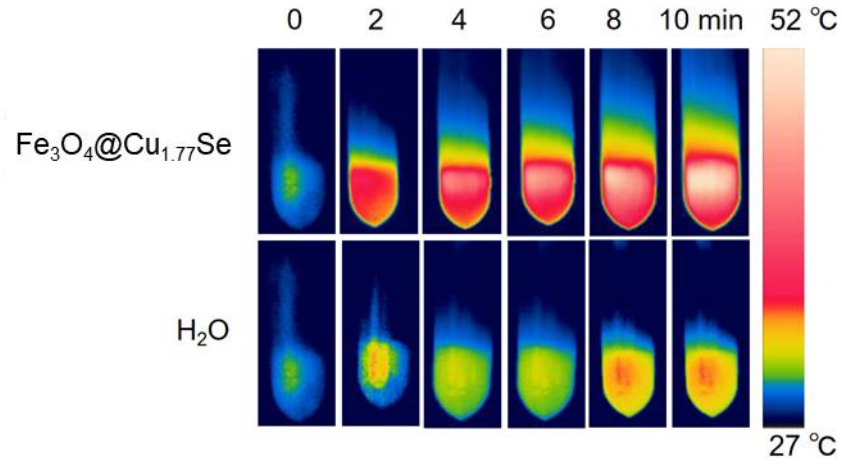

Figure S5. Thermal images of water (control) and $Fe_3O_4@Cu_{1.77}Se$ under second NIR photoirradiation (1064 nm, 0.75 W cm^{-2}).

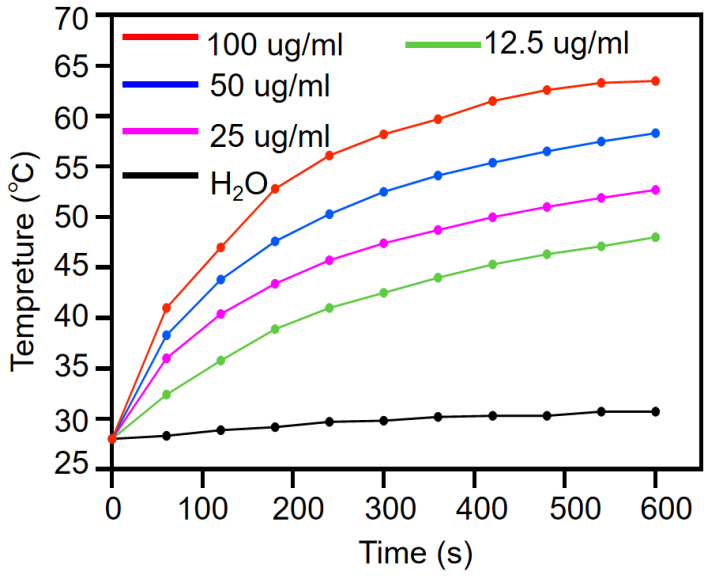

Figure S6. Temperature increase of water (control) and $Fe_3O_4@Cu_{1.77}Se$ with different concentrations under second NIR photoirradiation (1064 nm, 1.0 W cm^{-2}).

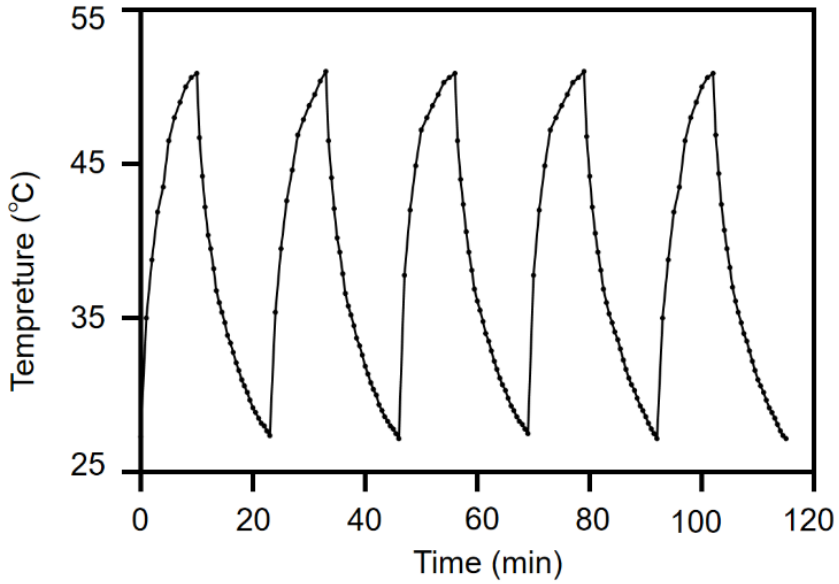

Figure S7. Photothermal stability of $Fe_3O_4@Cu_{1.77}Se$ nanozymes upon five cycling tests (50 μg mL^{-1}, 0.75 W cm^{-2}, 10 min).

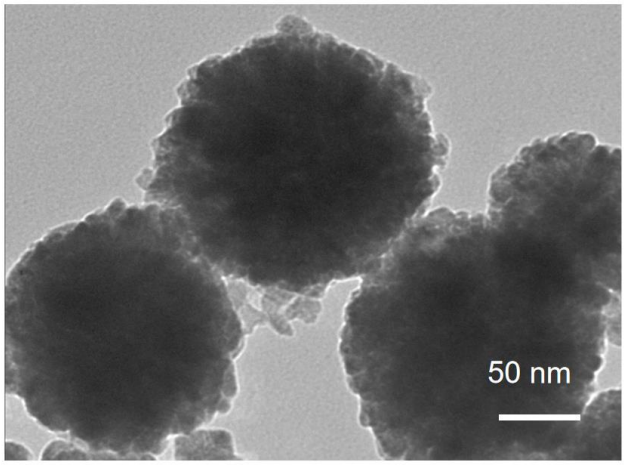

Figure S8. TEM image of Fe_3O_4@$Cu_{1.77}Se$ after photoirradiation for 5 cycles (1064 nm, 0.75 W cm^{-2}, 10 min).

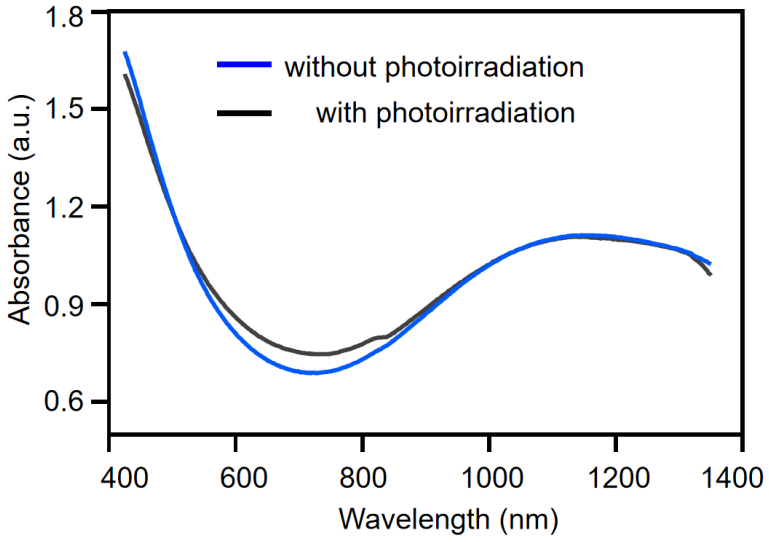

Figure S9. UV-visible-NIR spectra of Fe_3O_4@$Cu_{1.77}Se$+MMP-2 in the presence or the absence of photoirradiation.

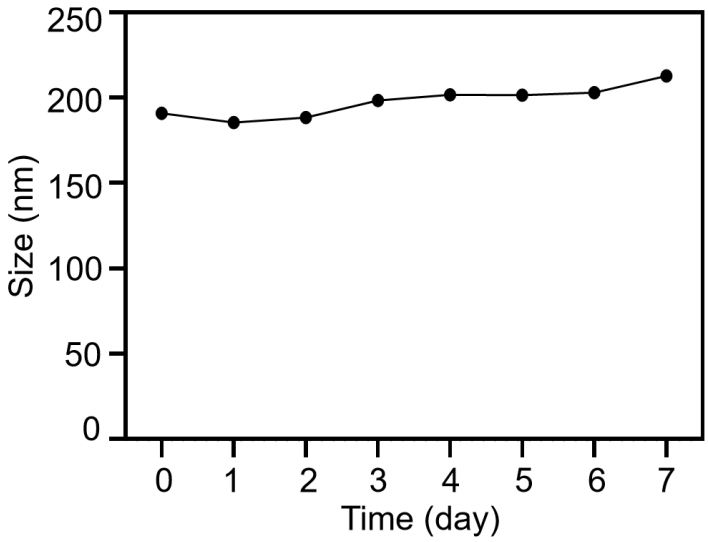

Figure S10. DLS profiles of Fe_3O_4@$Cu_{1.77}$Se-PEG nanozymes in PBS for 7 days.

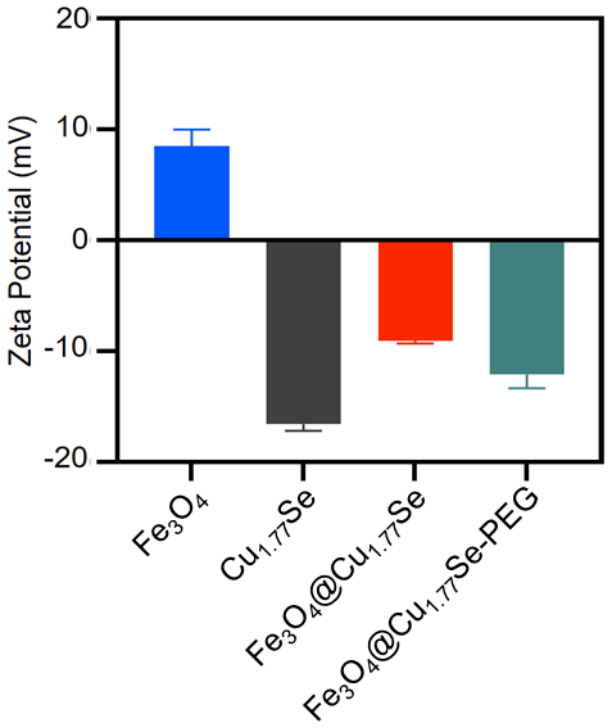

Figure S11. Zeta potentials of Fe_3O_4, $Cu_{1.77}Se$, Fe_3O_4@$Cu_{1.77}Se$ and Fe_3O_4@$Cu_{1.77}Se$-PEG.

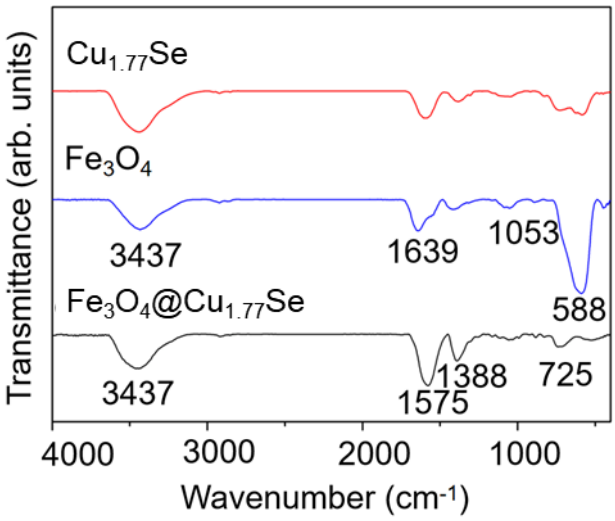

Figure S12. FTIR spectra of Fe_3O_4, $Cu_{1.77}Se$ and $Fe_3O_4@Cu_{1.77}Se$, respectively.

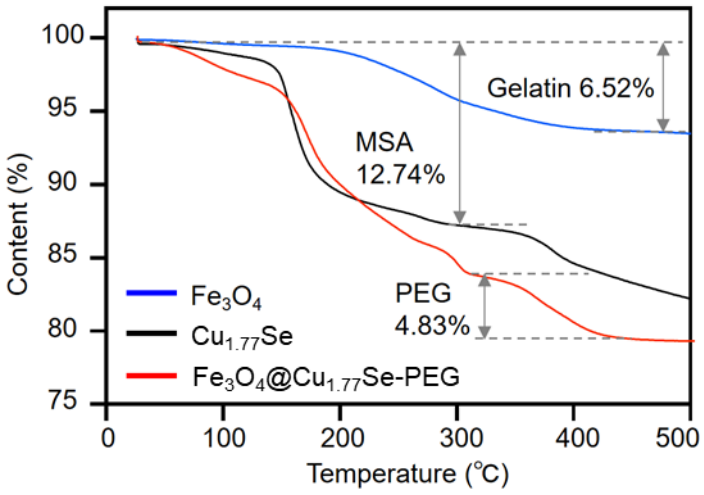

Figure S13. TGA curves of Fe_3O_4, $Cu_{1.77}Se$ and $Fe_3O_4@Cu_{1.77}Se$-PEG, respectively.

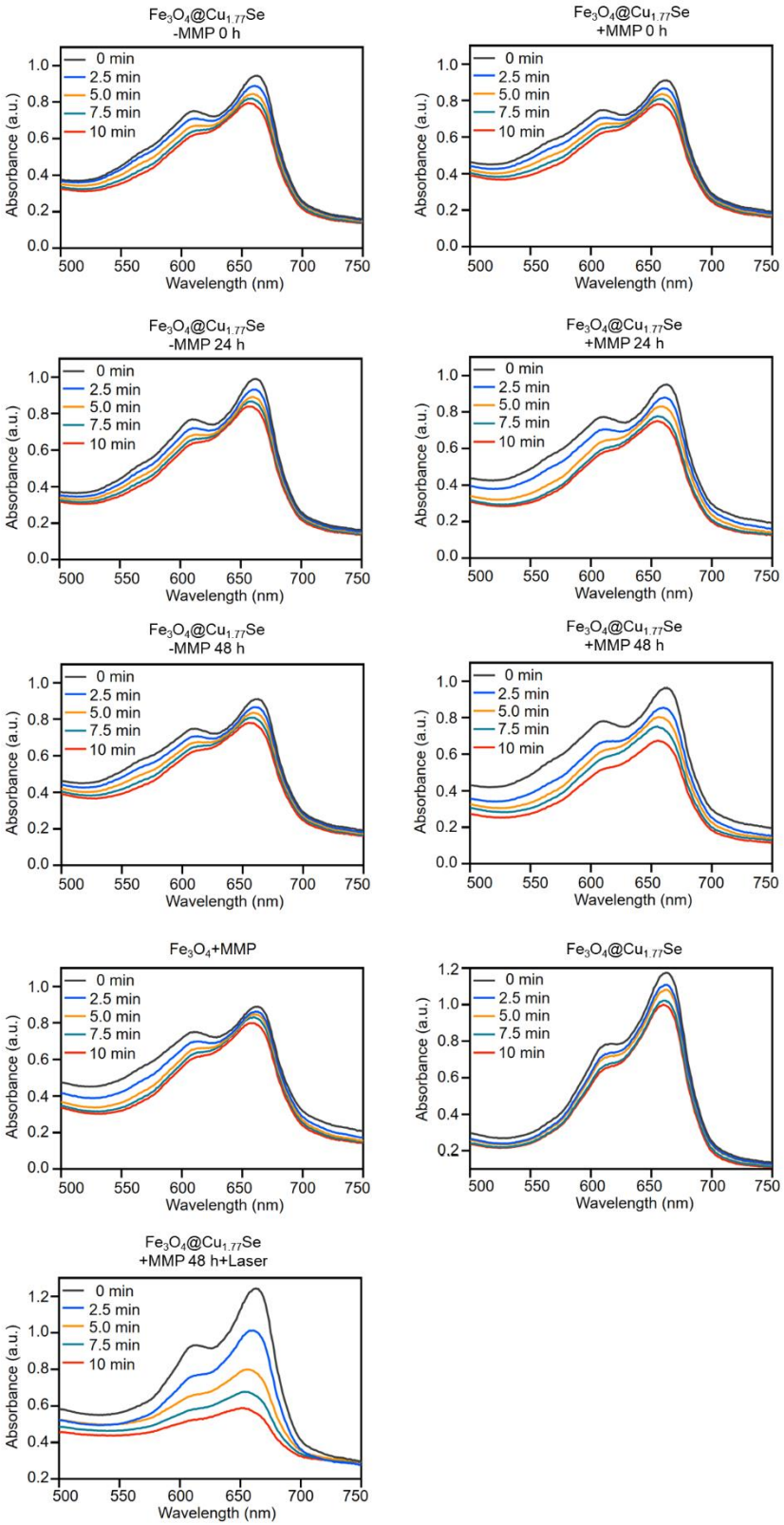

Figure S14. *In vitro* hydroxyl radicals production by Fe_3O_4, $Cu_{1.77}Se$, Fe_3O_4@$Cu_{1.77}Se$-MMP, Fe_3O_4@$Cu_{1.77}Se$+MMP and Fe_3O_4@$Cu_{1.77}Se$+MMP with laser irradiation (0.75 W cm^{-2}, 10 min).

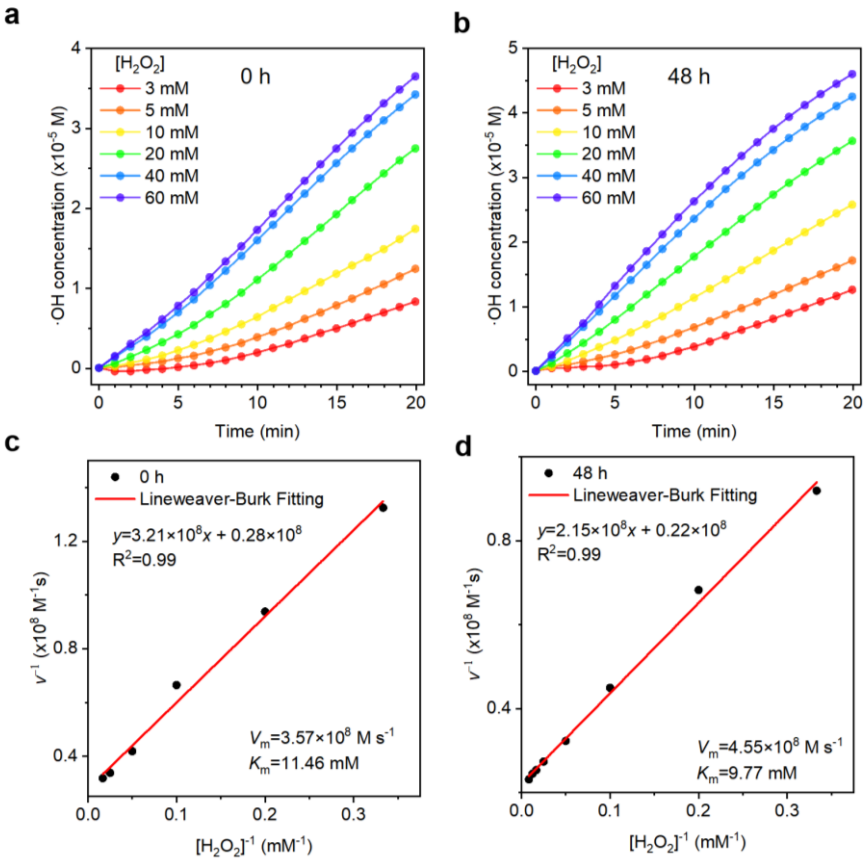

Figure S15. Time-dependent generation of ·OH of Fe_3O_4@$Cu_{1.77}Se$ incubated with MMP-2 for (a) 0 h and (b) 48 h in different concentration of H_2O_2/PBS solution. Lineweaver-Burk plotting for Fe_3O_4@$Cu_{1.77}Se$ incubated with MMP-2 for (a) 0 h or (b) 48 h.

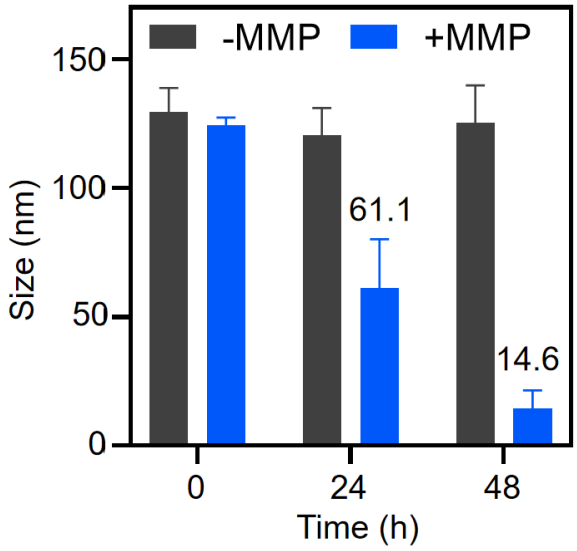

Figure S16. Size variation of Fe_3O_4@$Cu_{1.77}Se$ nanozymes upon treatment with MMP-2 at different time duration.

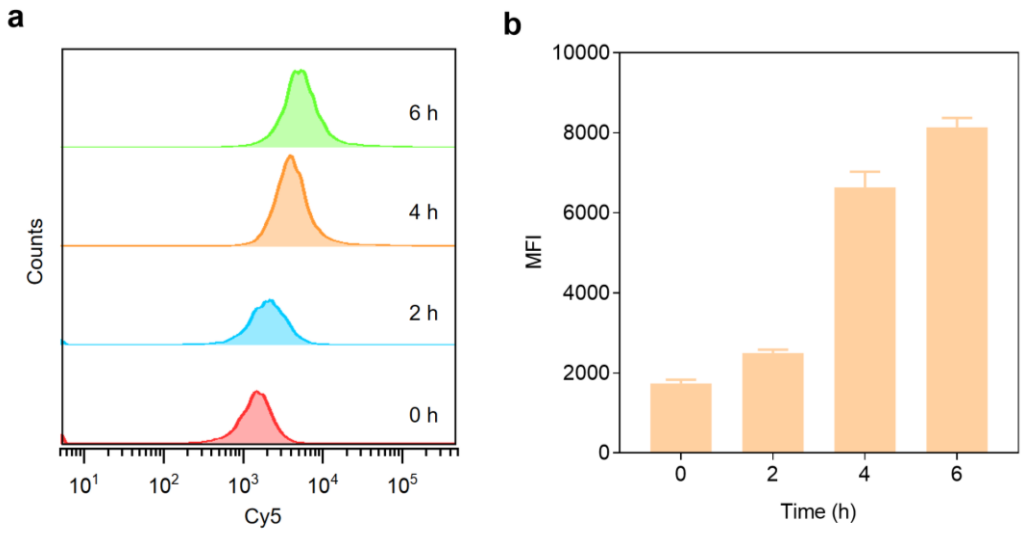

Figure S17. Cellular uptake of Fe_3O_4@$Cu_{1.77}Se$ by 4T1 cells after incubation for 0, 2, 4, and 6 h, respectively.

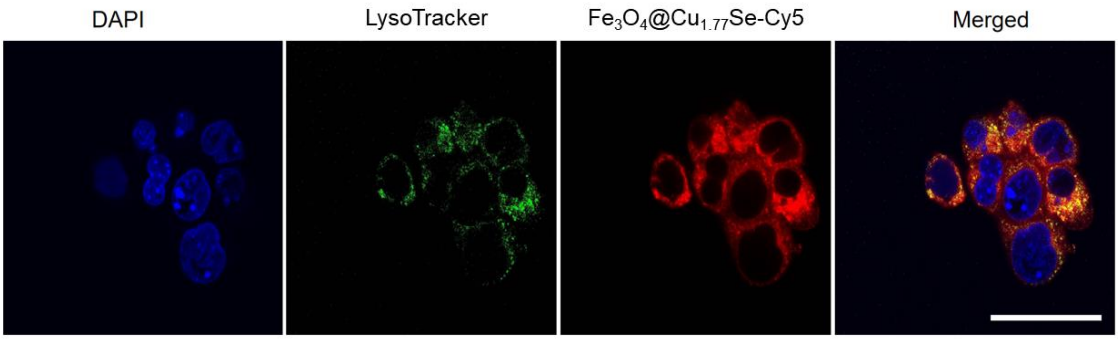

Figure S18. CLSM images of 4T1 cells incubated with Fe_3O_4@$Cu_{1.77}Se$ nanozymes for 4 h. Cell nuclei were stained with DAPI (blue color). Lysosomes were labeled with LysoTracker (green color). Scale bar: 50 μm.

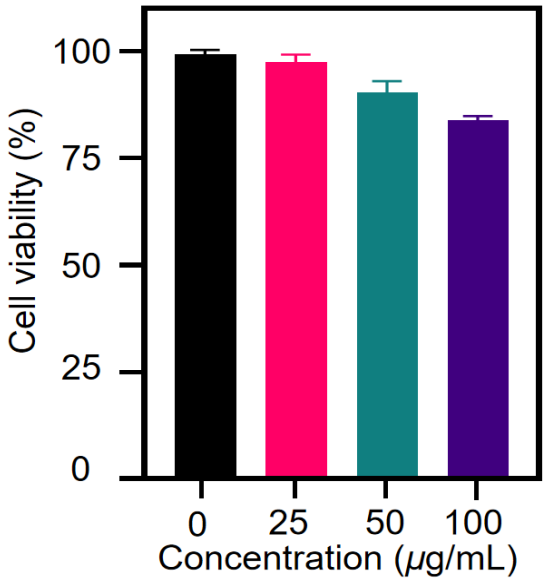

Figure S19. Cell viability of 4T1 cells after incubation with different concentration (0, 25, 50, and 100 μg mL^{-1}) of Fe_3O_4@$Cu_{1.77}Se$ nanozymes for 24 h.

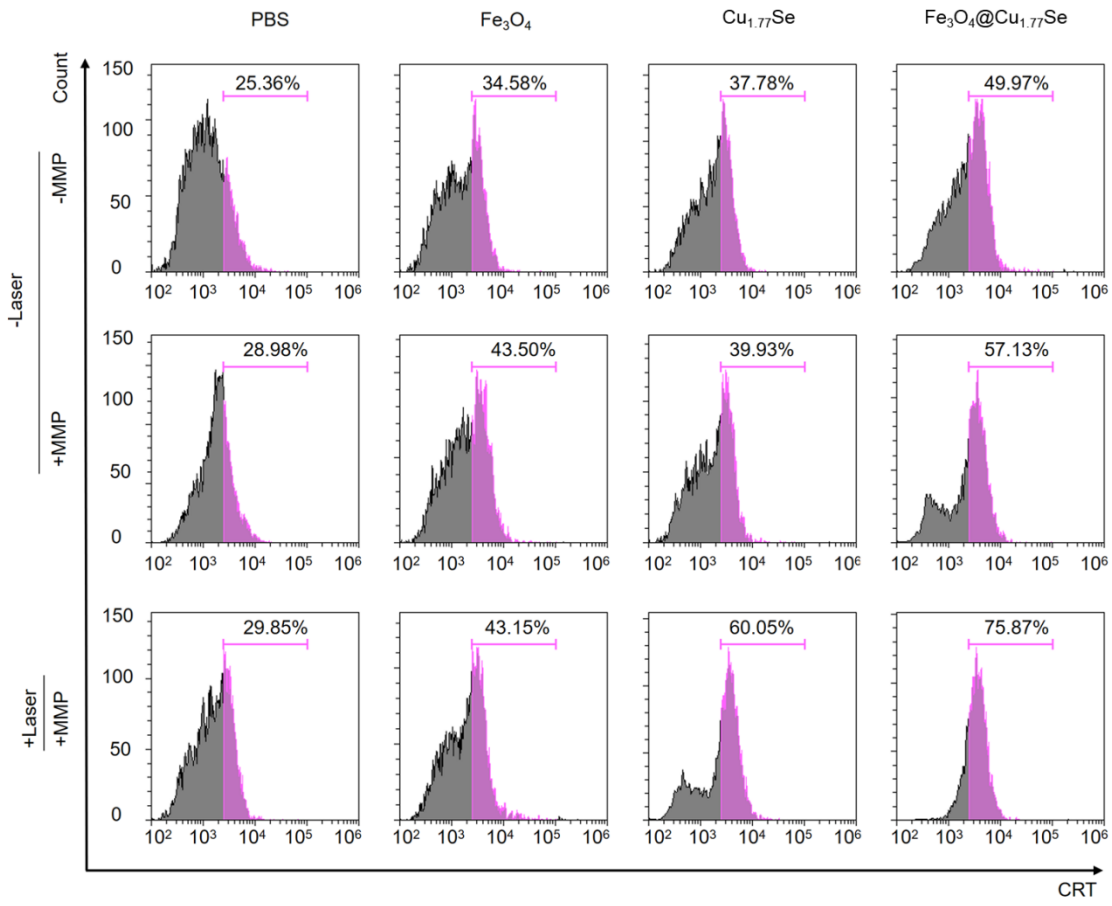

Figure S20. *In vitro* CRT expression after treatment by PBS, Fe_3O_4, $Cu_{1.77}Se$, $Fe_3O_4@Cu_{1.77}Se$ without MMP-2, with MMP-2, with MMP-2+ photoirradiation for 4 min (1064 nm, 0.75 W cm^{-2})

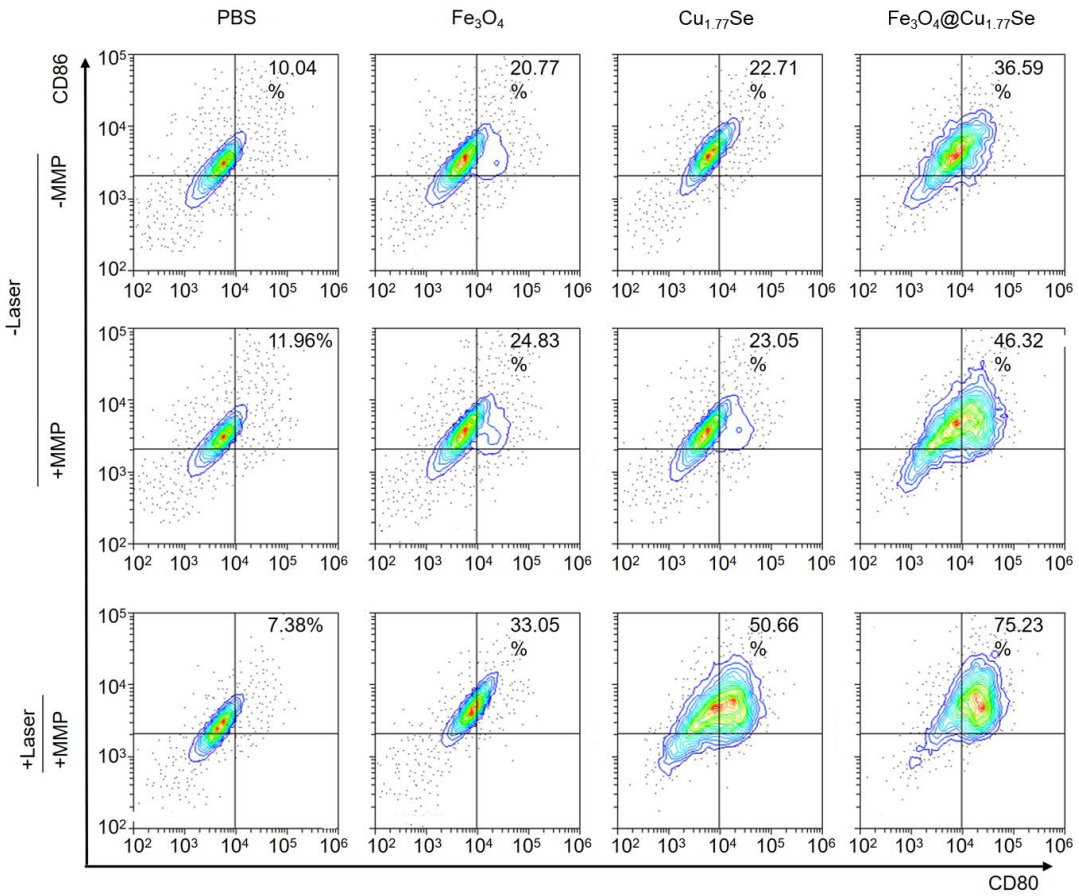

Figure S21. *In vitro* DCs maturation after treatments by PBS, Fe_3O_4, $Cu_{1.77}Se$, Fe_3O_4@$Cu_{1.77}Se$ without MMP-2, with MMP-2, with MMP-2 + photoirradiation for 3 min (1064 nm, 0.75 W cm^{-2}).

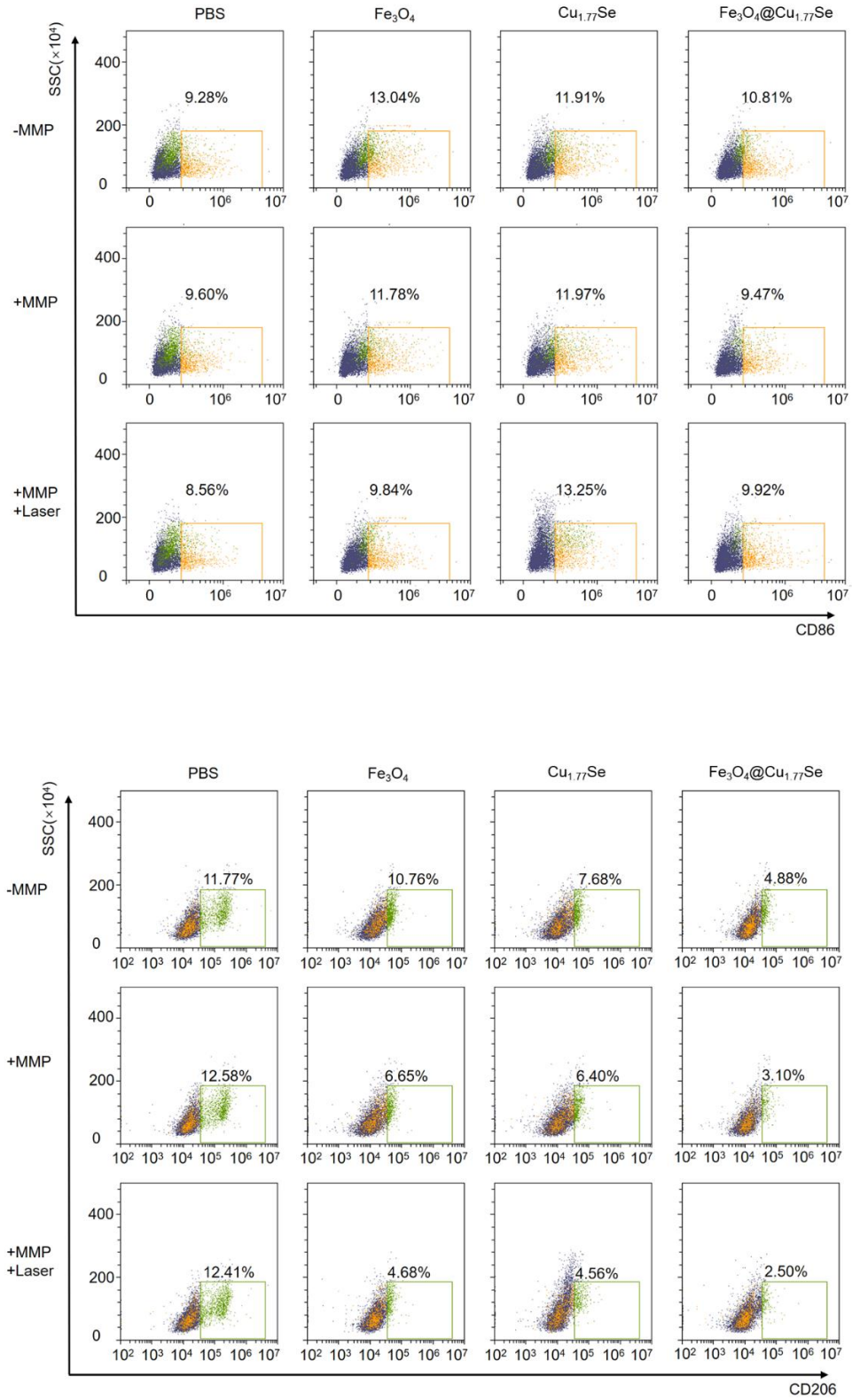

Figure S22. *In vitro* M1/M2-like TAMs after treatment by PBS, Fe_3O_4, $Cu_{1.77}Se$, $Fe_3O_4@Cu_{1.77}Se$ without MMP-2, with MMP-2, with MMP-2 + photoirradiation for 3 min (1064 nm, 0.75 W cm^{-2}).

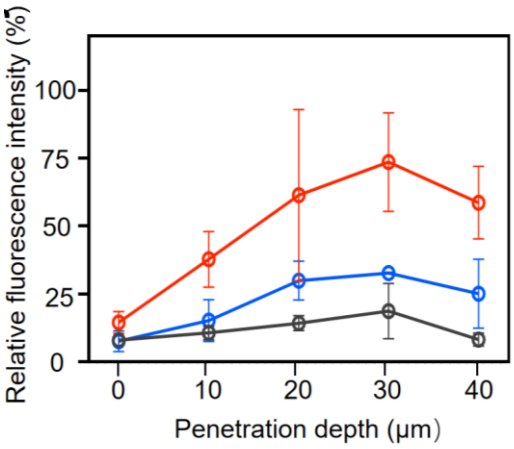

Figure S23. Quantification of 4T1 MCSs incubated with Fe_3O_4@$Cu_{1.77}$Se-Cy5 at concentration of 50 μg mL^{-1} without MMP-2, with MMP-2, with MMP-2 and photoirradiation for 4 min (1064 nm, 0.75 W cm^{-2}).

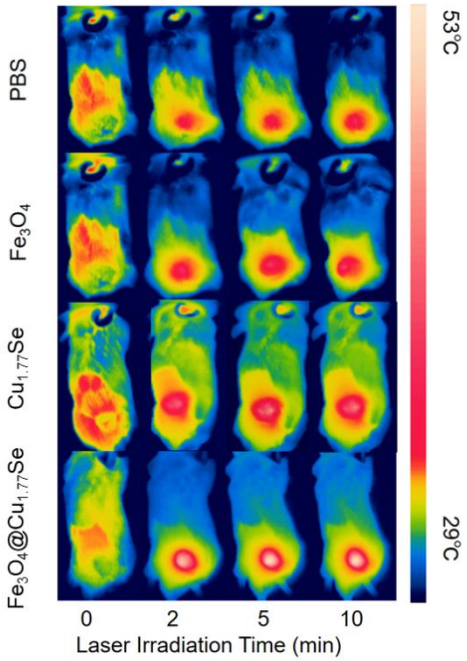

Figure S24. Thermal images at the tumor sites of the 4T1 tumor-bearing mice in different groups at different photoirradiation time.

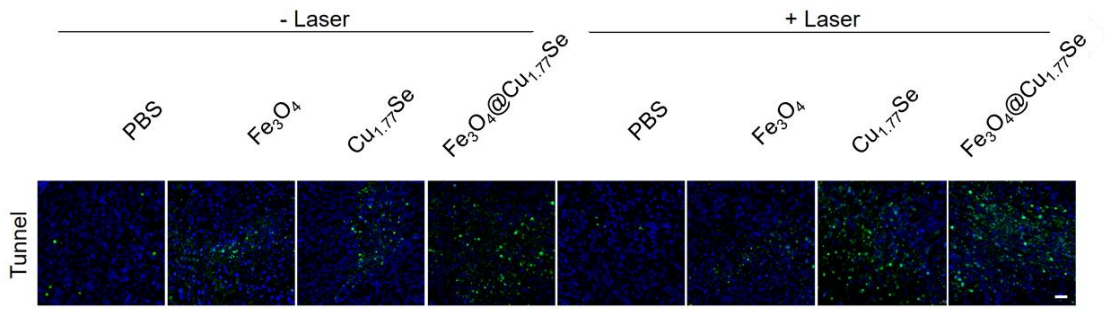

Figure S25. Tunnel staining in 4T1 tumors after treatments. Tumor cells necrosis were indicated with green false color. The cell nuclei stained with DAPI (blue color). Scale bar: 20 μm.

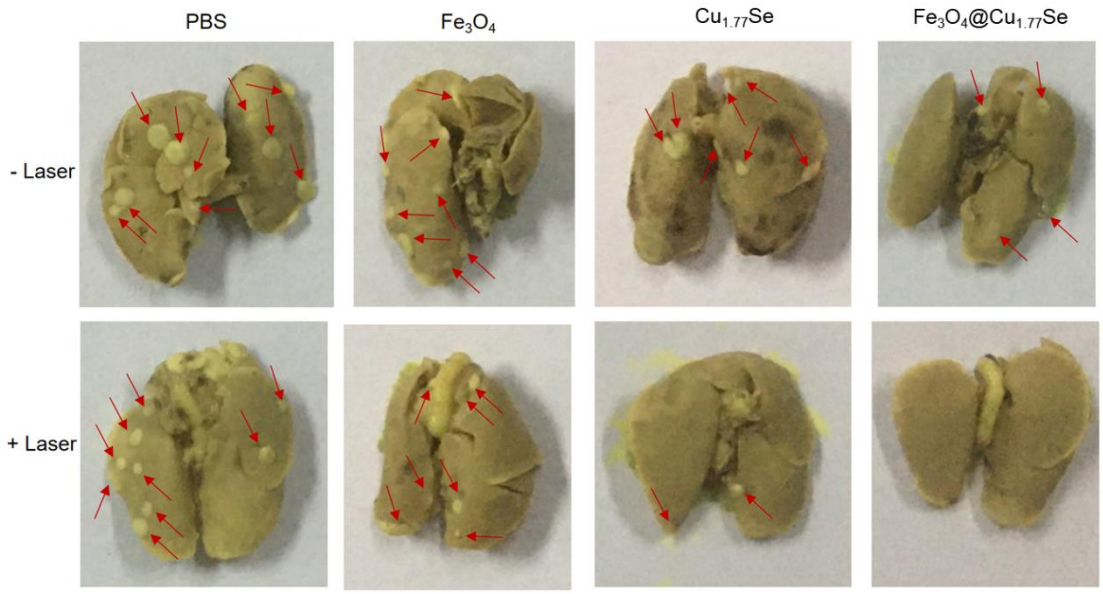

Figure S26. Images of metastasis nodules in lung of mice after treatments. Arrows indicate the metastasis nodules.

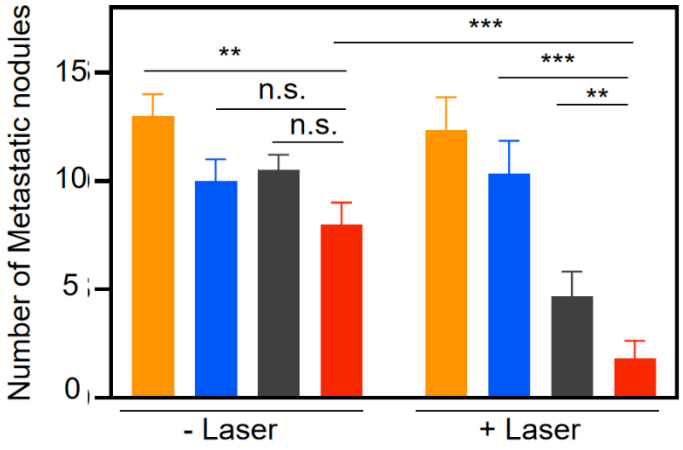

Figure S27. Number of metastasis nodules per lung in mice after treatments.

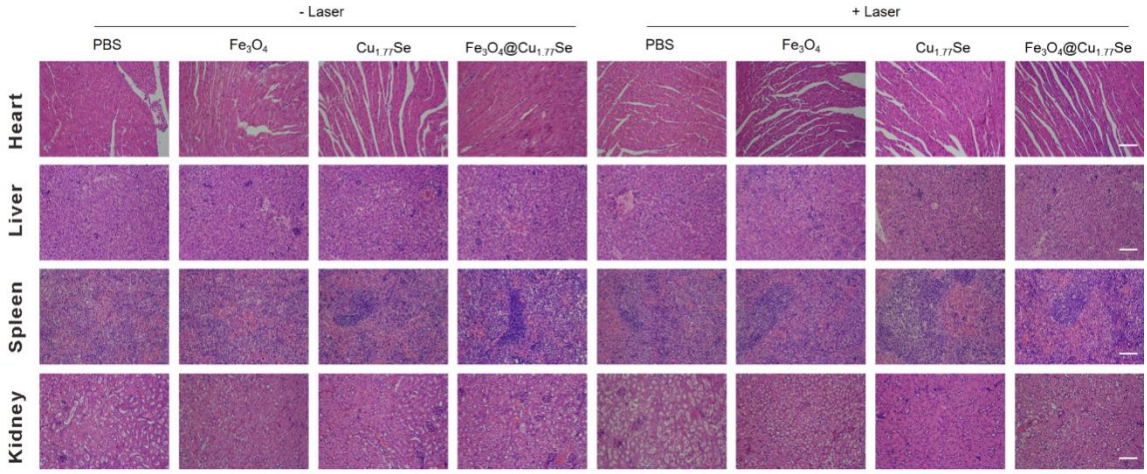

Figure S28. H&E staining of the main organs (heart, liver, spleen, and kidney) after treatments. Scale bar: 200 μm.

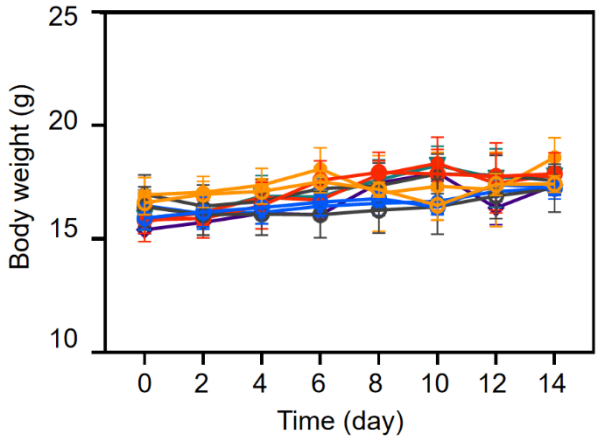

Figure S29. Body weight of 4T1 tumor-bearing mice after treatments.

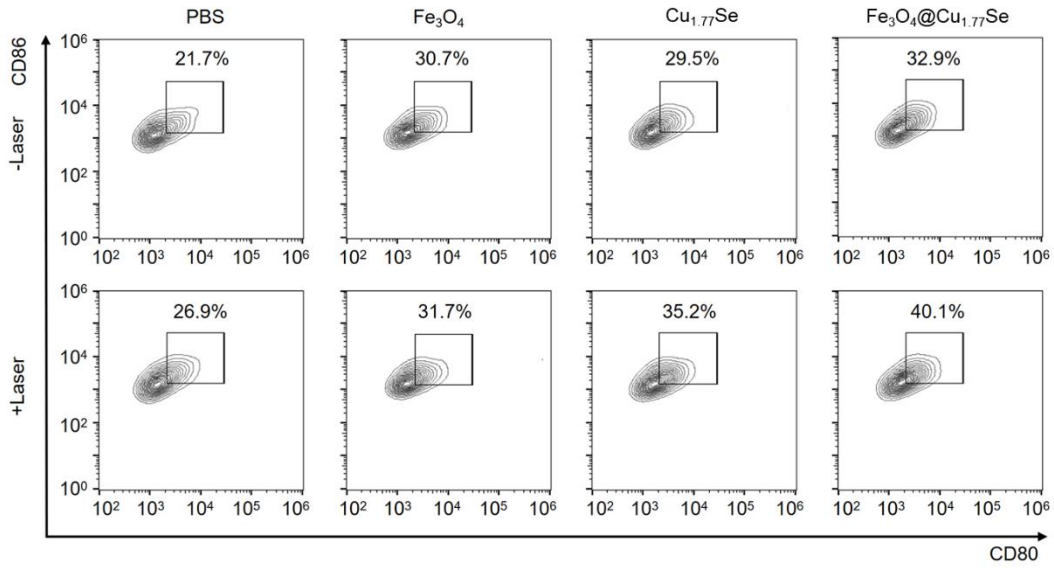

Figure S30. *In vivo* DCs maturation after treatment by PBS, Fe_3O_4, $Cu_{1.77}Se$, $Fe_3O_4@Cu_{1.77}Se$ without and with photoirradiation for 10 min (1064 nm, 0.75 W cm^{-2}).

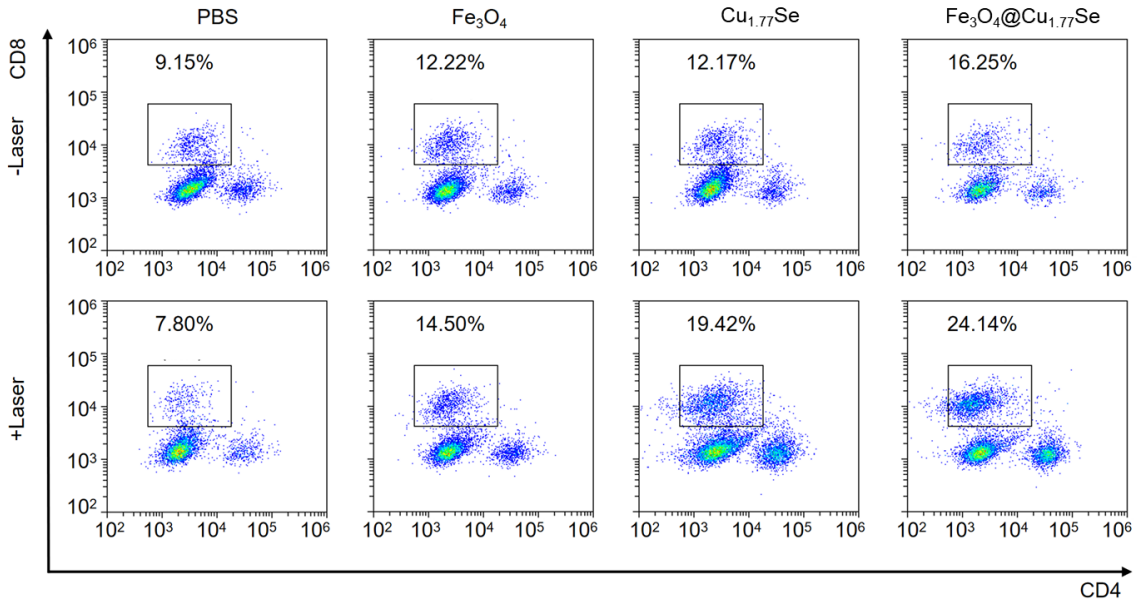

Figure S31. *In vivo* $CD8^+$ T cells in $CD45^+CD3^+$ T cells of 4T1 tumors after treatment by PBS, Fe_3O_4, $Cu_{1.77}Se$, $Fe_3O_4@Cu_{1.77}Se$ without and with photoirradiation for 10 min (1064 nm, 0.75 W cm^{-2}).

Reference:

1. L. Li, S. Fu, C. Chen, X. Wang, C. Fu, S. Wang, W. Guo, X. Yu, X. Zhang, Z. Liu, J. Qiu, H. Liu, *ACS Nano*, **2016**, 10, 7094-7105.
2. S. Zhang, C.Sun, J. Zeng, Q. Sun, G. Wang, Y. Wang, Y. Wu, S. Dou, M. Gao, Z. Li, *Adv Mater*, **2016**, 28, 8927-8936.
3. X. Wang, X. Zhong, H. Lei, Y. Geng, Q. Zhao, F. Gong, Z. Yang, Z. Dong, Z. Liu, L. Cheng, *Chem. Mater.*, **2019**, 31, 6174-6186.
4. W. Feng, X. Han, R. Wang, X. Gao, P. Hu, W. Yue, Y. Chen, J. Shi, *Adv Mater*, **2019**, 31, e1805919.
5. X. Tan, J. Huang, Y.Wang, S. He, L. Jia, Y. Zhu, K. Pu, Y. Zhang, X. Yang, *Angew. Chem. Int. Ed.*, **2021**, 60, 14051-14059.
6. D. Wang, Y. Yao, J. He, X. Zhong, B. Li, S. Rao, H. Yu, S. He, X. Feng, T. Xu, B. Yang, T. Yong, L. Gan, J. Hu, X. Yang, *Adv Sci*, **2020**, 7, 1901293.
7. J. Li, D. Cui, Y. Jiang, J. Huang, P. Cheng, K. Pu, *Adv Mater*, **2019**, 31, e1905091.